THE JOURNAL OF PHYSICAL CHEMISTRY B

Article

pubs.acs.org/JPCB

Quantitative Correlation of Counterion (X) Affinity to Ionic Micelles and X- and Temperature-Induced Micellar Growth (Spherical − Wormlike Micelles − Vesicles) for X = 5-Methyl- and 5-Methoxysalicylate Ions

Nor Saadah M. Yusof and M. Niyaz Khan*

Department of Chemistry, Faculty of Science, University of Malaya, 50603 Kuala Lumpur, Malaysia

Supporting Information

ABSTRACT: The semiempirical kinetic method has been used to determine the ratio of cetyltrimethylammonium bromide, CTABr, micellar binding constants of counterions X (K_X) and Br (K_{Br}), i.e., K_X/K_{Br} (= R_X^{Br}) for X = dianionic 5-methyl- and 5-methoxysalicylate ions. The values of K_X and K_{Br} have been derived from the kinetic parameters obtained in the presence of spherical/nonspherical and spherical micelles, respectively. The values of R_X^{Br} remain essentially independent of [CTABr] within its range 0.005−0.015 M for both dianionic 5-methyl- and 5-methoxysalicylate ions. The increase in temperature from 35 to 55 °C decreases the values of R_X^{Br} from 796 to 53 for 5-methylsalicylate ions and from 89 to 7.0 for 5-methoxysalicylate ions. Rheological properties of 0.015 M CTABr solutions containing ≥0.01 M counterionic salt, M_2X, show indirectly the presence of unilamellar vesicles, ULV, and long linear, entangled, and branched wormlike micelles, WM, at, respectively, 35 and 55 °C for X = dianionic 5-methylsalicylate ion. However, such studies show WM and probable spherical micelles, SM, at, respectively, 35 and 55 °C for X = dianionic 5-methoxysalicylate ions. It has been shown that, at a constant [CTABr], the micellar structural transitions from SM-to-WM-to-vesicles may be correlated quantitatively with the values of R_X^{Br} regardless of whether such micellar structural transitions occur due to variation in the values of [M_2X] at a constant temperature or due to variation in temperature at a constant [M_2X].

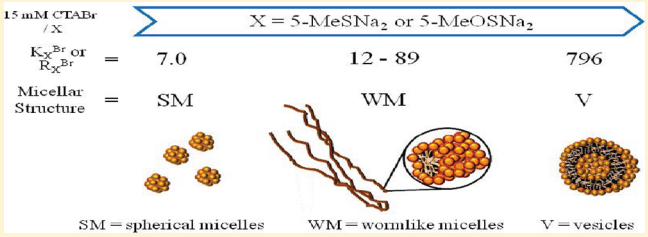

INTRODUCTION

It has been a general and widely accepted perception for nearly the last 35 years, based upon qualitative physicochemical evidence, that a strong counterion (X) binding with ionic micelles is the origin of X-induced micellar structural transition from spherical to viscoelastic/nonviscoelastic long linear and entangled wormlike micelles.[1−6] Recently, the efforts have been made to correlate qualitatively the X-induced ionic micellar structural growth in terms of specific interactions of X ions with ionic headgroups derived based upon Hofmeister anions[7] and a simple "law of matching water affinity" proposed by Collins.[8] The quantification of this perceived strong micellar binding of moderately hydrophobic counterions, X, such as benzoate and substituted benzoate ions, is almost completely lacking.[9] To find an answer to the question "what interactions cause wormlike micelles to grow from spherical micelles?", Lin et al.[10] carried out cryo-TEM as well as rheological measurements on aqueous solutions containing 0.02 M CTABr and different concentrations of 5-methylsalicylic acid, 5-MeSaH. Incidentally, these authors found the presence of unilamellar vesicles (ULV) at [5-MeSaH]/[CTABr] ≈ 1.1. In the subsequent studies, the presence of ULV was found in aqueous solutions of CTABr mixed with sodium 3-methylsalicylate[11] and CTA5ES (5ES represents 5-ethylsalicylate).[12] In some of these studies,[11−13] vesicle-to-wormlike micelle transitions with increasing temperature have been observed. A more systematic study with the CTABr−5-MeSaH system has been carried out by employing a combination of visual observations, turbidimetry, rheological techniques, and small-angle neutron scattering, SANS, measurements, and these studies demonstrated unambiguously the formation of probable ellipsoidal[14] micelles, long linear and entangled wormlike micelles, and ULV under different conditions in terms of temperature and [5-MeSaH]/[CTABr].[15] However, in the absence of the knowledge of the values of micellar binding constants of counterion in all these studies,[11−13,15] the results were rationalized qualitatively in view of the importance of the binding of the micellar counterions on the micellar structural transitions.

The counterion, X, affinity to ionic micelles can be measured quantitatively by determining the value of ion exchange constant, K_X^Y, where Y represents a reference counterion, say Br^-. However, the reported values of K_X^Y for Y = Cl^- or Br^- and X = substituted benzoate ions are only a few.[16] A recent semiempirical kinetic, SEK, method has been used to determine K_X^{Br} or R_X^{Br} (with $R_X^{Br} = K_X/K_{Br}$ where the values of CTABr micellar binding constants, K_{Br} and K_X, have been derived from

Received: October 31, 2011
Revised: January 18, 2012
Published: January 24, 2012

   dx.doi.org/10.1021/jp210467p | J. Phys. Chem. B 2012, 116, 2065−2074

kinetic parameters obtained in the presence of spherical and nonspherical micelles, respectively).[16,17] Thus, in the SEK method, $R_X^{Br} = K_X^{Br}$ when the value of K_X has been derived from kinetic parameters obtained in the presence of spherical micelles. Here, in this paper, we report the following studies: (i) the SEK method has been used to determine the values of K_X^{Br} or R_X^{Br} for X = dianionic 5-methylsalicylate, 5-$MeSa^{2-}$, and 5-methoxysalicylate, 5-$MeOSa^{2-}$, ions at different temperature and (ii) the rheometric measurements have been carried out on aqueous CTABr−M_2X solutions with M_2X = 5-$MeSaNa_2$ and 5-$MeOSNa_2$, at a constant value of [CTABr] and different values of [M_2X] and temperature. The observed results and their probable explanations are described in this manuscript.

EXPERIMENTAL SECTION

Reagent-grade chemicals such as 5-methylsalicylic acid, 5-MeSaH, 5-methoxysalicylic acid, 5-MeOSaH, cetyltrimethylammonium bromide, CTABr, phenyl salicylate, PSaH, and piperidine, Pip, were commercial products of highest available purity. All other common chemicals used were also of reagent grade. The stock solutions of 0.5 M M_2X (= 5-$MeSaNa_2$ and 5-$MeOSaNa_2$) were prepared by adding 1.05 M NaOH to the corresponding 0.5 M solutions of 5-MeSaH or 5-MeOSaH. The stock solutions of 0.01 M PSaH were prepared in acetonitrile.

Determination of K_X^{Br} or R_X^{Br} for Different X (= 5-$MeSa^{2-}$ and 5-$MeOSa^{2-}$) by the Use of the SEK Method. The SEK method uses an appropriate reaction kinetic probe in the experimental determination of K_X^{Br} or R_X^{Br}.[17] The effects of the concentrations of nonreactive salts of different counterions, [MX], on pseudofirst-order rate constants, k_{obs}, for the nucleophilic reaction of Pip with ionized phenyl salicylate, PSa^-, in the absence and presence of CTABr micelles have been used as the kinetic probe for the use of the SEK method. The determination of K_X^{Br} or R_X^{Br}, by the use of the SEK method, requires the values of kinetic parameters, $K_{X/S}^n$, for X = X^- (test counterions) and Br^- (reference counterion), at a constant $[CTABr]_T$ and temperature. The values of $K_{X/S}^n$ were determined by the use of K_S^0 (= CTABr micellar binding constant of PSa^- at [MX] = 0 with M = Na^+) and by the use of pseudofirst-order rate constants, k_{obs}, for the nucleophilic reactions of piperidine with PSa^-, determined at constant $[CTABr]_T$ and temperature as well as different values of [M_2X] (M_2X = 5-$MeSaNa_2$, 5-$MeOSaNa_2$, and MX = NaBr). The values of $K_{Br/S}^n$ and K_S^0 are known at 35 °C[16] but unknown at 40, 45, and 55 °C. The value K_S^0, at a constant temperature, was determined by studying the effects of $[CTABr]_T$ on k_{obs} at [MX] = 0. The use of the SEK method also requires the values of k_{obs} at different values of [MX] at $[CTABr]_T$ = 0. The details of the SEK method and the reaction kinetic probe are described in earlier reports.[16−18]

Kinetic and Rheometric Measurements. The rate of piperidinolysis of PSa^-, in the absence and presence of a constant total concentration of CTABr, $[CTABr]_T$, with $[CTABr]_T$ > cmc where cmc is the critical micelle concentration, and M_2X, [M_2X], was monitored spectrophotometrically at an appropriate constant wavelength and temperature. The experimental details of the reaction rate measurements and kinetic data analysis are the same as described in the recent report.[19] Rheological measurements were carried out by the use of a Brookfield R/S+ rheometer with double gap coaxial cylinder, CC-DG, and the experimental details could be found elsewhere.[19]

RESULTS

Effects of [M_2X] on Pseudofirst-Order Rate Constants (k_{obs}) for the Nucleophilic Reaction of Pip with PSa^- at a Constant $[CTABr]_T$ and Temperature. Several kinetic runs were carried out at different values of [M_2X], within 0 ≤ [M_2X] ≤ 0.070 M for M_2X = 5-$MeSaNa_2$ and 0 ≤ [M_2X] ≤ 0.10 M for M_2X = 5-$MeOSaNa_2$, at a constant $[CTABr]_T$, 0.1 M Pip, 2 × 10^{-4} M PSa^- (if λ = 350 nm) or 4 × 10^{-4} M PSa^- (if λ = 380 nm), and 35 °C. The values of [NaOH] were varied from 0.030 to ≤0.035 M under the experimental conditions of entire kinetic runs. The values of k_{obs} at different [M_2X] and within the $[CTABr]_T$ range 0.005−0.015 M are shown graphically by Figures 1 and 2 for, respectively, M_2X = 5-$MeSaNa_2$ and 5-$MeOSaNa_2$. Similar observations were also obtained at 40, 45, and 55 °C for M_2X = 5-$MeSaNa_2$ and 5-$MeOSaNa_2$. The values of k_{obs} as a function of [M_2X] at 0.005 and 0.0125 M CTABr as well as at 40, 45, and 55 °C are shown by the plots of Figures S1 and S2 of Supporting Information (SI) for, respectively, M_2X = 5-$MeSaNa_2$ and 5-$MeOSaNa_2$.

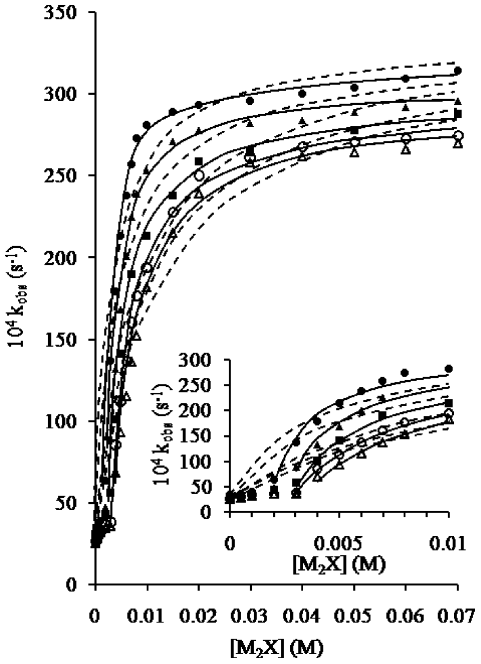

Figure 1. Plots showing the dependence of k_{obs} upon [M_2X], M_2X = 5-$MeSaNa_2$, for piperidinolysis of PSa^- at 2 × 10^{-4} M PSa^-, 0.1 M Pip, 35 °C, and $[CTABr]_T/M$ = 0.005 (●), 0.007 (▲), 0.010 (■), 0.0125 (○), and 0.015 (Δ). The dashed lines are drawn through the calculated data points with kinetic parameters, k_0, θ, and $K^{X/S}$, listed in Table S2 (SI), at $[M_2X]_0^{op}$ = 0. The solid lines are drawn through the calculated data points with kinetic parameters, k_0, θ, and $K^{X/S}$, listed in Table S2 (SI), at $[M_2X]_0^{op}/M$ = 0.0018 (●), 0.0025 (▲), 0.0027 (■), 0.0028 (○), and 0.0032 (Δ). Inset: The plots at magnified scale for the data points at the lower values of [M_2X].

Effects of [NaBr] on k_{obs} for the Nucleophilic Reaction of Pip with PSa^- at a Constant $[CTABr]_T$ and Temperature. The effects of [NaBr] on k_{obs} for piperidinolysis of PSa^-, at a constant $[CTABr]_T$ and temperature, were studied to determine a kinetic parameter needed to calculate the value of R_X^{Br} at a temperature other than 35 °C because the value of this kinetic parameter is known at 35 °C. The values of k_{obs} at different [NaBr] were obtained by carrying out kinetic runs within the [NaBr] range 0.05−1.50 at 0.005 M CTABr, 0.1 M

dx.doi.org/10.1021/jp210467p | J. Phys. Chem. B 2012, 116, 2065−2074

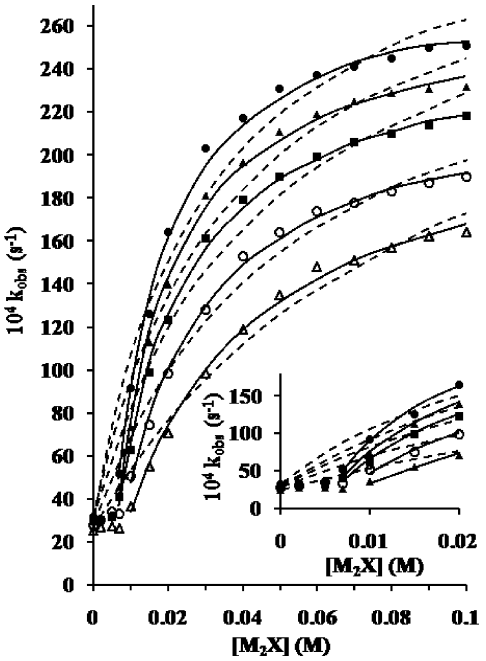

Figure 2. Plots showing the dependence of k_{obs} upon [M_2X], M_2X = 5-MeOSaNa$_2$, for piperidinolysis of PSa^- at 4 × 10^{-4} M PSa^-, 0.1 M Pip, 35 °C, and [CTABr]$_T$/M = 0.005 (●), 0.007 (▲), 0.010 (■), 0.0125 (○), and 0.015 (Δ). The dashed lines are drawn through the calculated data points with kinetic parameters, k_0, θ, and $K^{X/S}$, listed in Table S2 (SI), at [M_2X]$_0^{op}$ = 0. The solid lines are drawn through the calculated data points with kinetic parameters, k_0, θ, and $K^{X/S}$, listed in Table S2 (SI), at [M_2X]$_0^{op}$/M = 0.0060 (●), 0.0062 (▲), 0.0064 (■), 0.0076 (○), and 0.0084 (Δ). Inset: The plots at magnified scale for the data points at the lower values of [M_2X].

Pip, 2 × 10^{-4} M PSa^-, and 40 °C. The values of k_{obs}, obtained under such conditions, are shown as the plots of k_{obs} vs [NaBr] in Figure S3 (SI). Similar observations were obtained at 45 and 55 °C, and these observations, obtained at 0.005 and 0.0125 M CTABr, are also shown graphically by Figure S3 (SI).

Effects of [M_2X] or [MX] on k_{obs} for the Nucleophilic Reaction of Pip with PSa^- in the Absence of CTABr. One of the requirements of the SEK method is to determine the effects of [M_2X] on k_{obs} at [CTABr]$_T$ = 0. Thus, a few kinetic runs were carried out for the nucleophilic reaction of Pip with PSa^- under the appropriate reaction conditions in the absence of CTABr. The least-squares calculated values of kinetic parameters, k_{obs}, δ_{ap} (molar extinction coefficient of reaction mixture), and A_∞ (observed absorbance at the reaction, t = ∞), at different values of [M_2X], M_2X = 5-MeSaNa$_2$, 5-MeOSaNa$_2$, and MX = NaBr are shown in Table S1 (SI). The values of k_{obs} remain independent of [M_2X] within its range 0.0−0.10 M for M_2X = 5-MeSaNa$_2$ and 5-MeOSaNa$_2$, while the values of k_{obs} decrease ∼17.2, 29.1, and 23.1% at the respective 40, 45, and 55 °C with the increase of [NaBr] from 0.0 to 1.5 M (Table S1, SI).

Effects of [CTABr]$_T$ on k_{obs} for the Nucleophilic Reaction of Pip with PSa^- in the Absence of MX or M_2X. The values of CTABr micellar binding constants (K_S^0) of PSa^- at 40, 45, and 55 °C and [MX] = 0 are not known, and these values of K_S^0 are needed in the determination of R_X^{Br} at these temperatures. To determine the value of K_S^0 at a constant temperature, nearly 20 kinetic runs were carried out at 2 × 10^{-4} M PSa^-, 0.03 M NaOH, 0.10 M Pip, 40 °C, and within [CTABr]$_T$ range 0.0−0.05 M. Similar observations were obtained at 45 and 55 °C. The values of k_{obs} at different values of [CTABr]$_T$ are shown graphically by Figure S4 (SI).

Rheological Observations of Aqueous Solutions of CTABr Containing 2 × 10^{-4} M PSa^-, 0.1 M Pip, and a Constant Value of [NaOH] and [M_2X]. Rheological measurements of aqueous solutions of mixed CTABr−M_2X, M_2X = 5-MeSaNa$_2$ and 5-MeOSaNa$_2$, were performed under the reaction conditions of kinetic measurements as well as steady-shear rheological response at 35 ± 1 °C. The values of shear viscosity (η) at different shear rates ($\dot{\gamma}$) were obtained at the constant values of [CTABr] (= 0.0125 M) and [M_2X]. These observations are shown as the log−log plots of η vs $\dot{\gamma}$ at different values of [M_2X] in Figures 3a and 4 for, respectively,

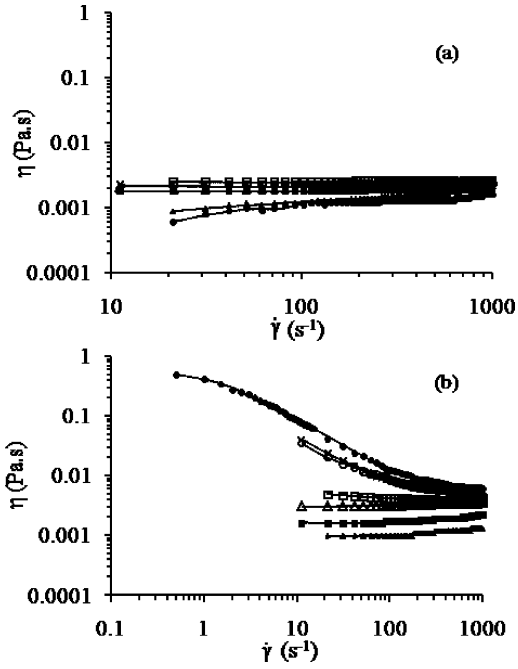

Figure 3. Plots showing the dependence of shear viscosity, η, vs shear rate, $\dot{\gamma}$, for samples with [CTABr]$_T$ = 0.0125 M and [5-MeSaNa$_2$]/M = (a) 0.005 (●), 0.007 (▲), 0.01 (■), 0.0125 (Δ), 0.02 (○), 0.04 (×), and 0.07 (□) at 35 °C and (b) 0.005 (▲), 0.007 (■), 0.01 (○), 0.0125 (●), 0.02 (×), 0.04 (□), and 0.07 (Δ) at 55 °C.

M_2X = 5-MeSNa$_2$ and 5-MeOSNa$_2$. Similar observations were also obtained at 40, 45, and 55 °C for M_2X = 5-MeSaNa$_2$ and 5-MeOSaNa$_2$, and these results are shown graphically by Figure 3b for data at 55 °C and Figure S5 (SI) for data at 40 and 45 °C. Figure S6 (SI) exhibits the plots of η vs $\dot{\gamma}$ at 0.0125 M CTABr, 40, 45, and 55 °C as well as different values of [M_2X] for M_2X = 5-MeOSaNa$_2$. The flow curves (i.e., plots of η vs $\dot{\gamma}$) were also obtained at 0.005 M CTABr mixed with different values of [M_2X] for M_2X = 5-MeSaNa$_2$ at 35 and 55 °C, and these results are shown graphically by Figure S7 (SI).

■ DISCUSSION

The rate of hydrolysis of phenyl salicylate is independent of [HO^-] within its range ∼0.005−0.06 M, and under such conditions, the rate of hydrolysis involves PSa^- and H_2O as the reactants.[20] Nucleophilic reactions of primary and secondary amines with PSa^- involve intramolecular general base assistance. The detailed mechanisms of these reactions have been described elsewhere.[21] The presence of micelles generally affects the rates of reactions without changing their aqueous

dx.doi.org/10.1021/jp210467p | J. Phys. Chem. B 2012, 116, 2065−2074

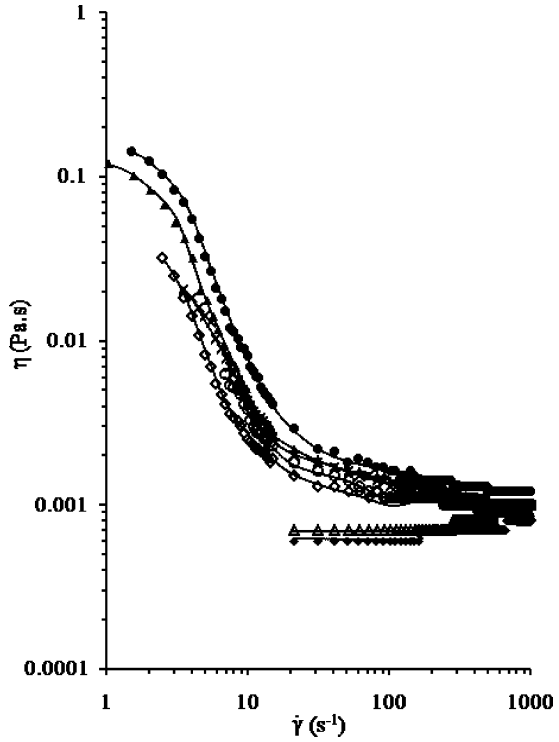

Figure 4. Plots showing the dependence of shear viscosity, η, vs shear rate, $\dot{\gamma}$, for samples with $[CTABr]_T$ = 0.0125 M and $[5\text{-MeOSaNa}_2]/M$ = 0.005 (◆), 0.010 (◇), 0.015 (▲), 0.020 (●), 0.040 (×), 0.070 (○), and 0.1 (Δ) at 35 °C.

phase reaction mechanisms. The effects of [CTABr] on k_{obs} for piperidinolysis of PSa^- could not reveal, at least indirectly, a change in the reaction mechanism. Spectrophotometric evidence[22] revealed the presence of nearly 100% PSa^- under the experimental conditions of entire kinetic runs of the present study. The rate of hydrolysis is negligible compared to that of piperidinolysis of PSa^- under the experimental conditions of entire kinetic runs of the present study.[23] In view of these observations, a brief reaction mechanism for the cleavage of PSa^-, under the present experimental conditions, may be expressed by Scheme 1. The symbol k^2 (Scheme 1) represents

Scheme 1

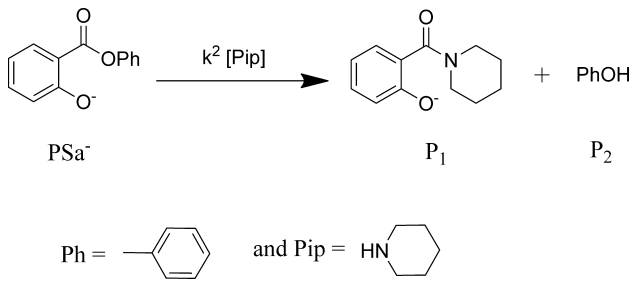

the nucleophilic second-order rate constant for the reaction of Pip with PSa^- and $[Pip]_T = [Pip] + [PipH^+] \approx [Pip]$ because $[PipH^+] \approx 0$ under the typical conditions of the present study.[23b,24] This fact is also evident from k_{obs} values summarized in Table S1 (SI).

Determination of K_S^0 at 40, 45, and 55 °C. The monotonic decrease of k_{obs} with the increase of $[CTABr]_T$, as shown in Figure S4 (SI), is similar to that obtained earlier in the absence and presence of NaBr.[23] These observed data were found to fit to eq 1 which has been derived by the use of the pseudophase micellar (PM) model.[23] A brief derivation of eq 1, in terms of the PM model, is described in the SI where all the symbols are explained in the Appendix.

$$k_{obs} = \frac{k_W + k_M K_S([CTABr]_T\text{-cmc})}{1 + K_S([CTABr]_T\text{-cmc})} \quad (1)$$

The observed data of Figure S4 (SI) were treated with eq 1 with $K_S = K_S^0$ because [NaBr] = 0, and the least-squares calculated values of k_M and K_S^0, at different temperatures, are summarized in Table 1. The value k_W, at constant temperature, was obtained experimentally by carrying out kinetic run(s) at $[CTABr]_T$ = 0. The values of cmc, critical micelle concentration, at a constant temperature were determined by kinetic iterative[25] and Broxton's graphical[26] techniques. The values of cmc, determined from iterative and graphical techniques, are not appreciably different from each other at a constant temperature. The calculated values of k_W and cmc, at different temperatures, are shown in Table 1. The observed data fit to eq 1 is considered to be satisfactory in view of the standard deviations of k_M and K_S^0 and the plots of Figure S4 (SI) where solid lines are drawn through the calculated data points. The plausible explanation(s) for the values of k_W/k_M (Table 1) could be found in the earlier reports.[23]

Determination of $K_{Br/S}^n$ at 40, 45, and 55 °C. It has been described in the earlier reports[12−15] that the nonlinear increase of k_{obs} with an increase of the concentrations of inert counterionic salts ([MX]) at the constant $[CTABr]_T$ (such as the data exhibited by Figure S3, SI) is due to the transfer of micelle-bound PSa^- ions (i.e., PSa^-_M) to the water phase (i.e., PSa^-_W) through the occurrence of the ion exchange process X^-/PSa^-. The values of k_{obs} at different [MX] (MX = NaBr) and at the constants $[CTABr]_T$ and $[Pip]_T$ (= 0.1 M) were found to fit to empirical eq 2

$$k_{obs} = \frac{k_0 + F_{X/S} k_W^{MX} K^{X/S}[MX]}{1 + K^{X/S}[MX]} \quad (2)$$

where $F_{X/S}$ and $K^{X/S}$ are empirical constants, and $k_0 = k_{obs}$ at [MX] = 0 but $[CTABr]_T \neq 0$ and $k_W^{MX} = k_{obs}$ at [MX] ≠ 0 but $[CTABr]_T$ = 0. Equation 2 has been found to explain the observed data in the related reaction systems where the values of k_{obs} showed significant sensitivity to [MX] at $[CTABr]_T$ = 0.[17a,27] The nonlinear least-squares technique was used to calculate the values of $F_{X/S}$ and $K^{X/S}$ from eq 2 considering k_0 and k_W^{MX} as the known parameters. These calculated results, obtained at different temperatures, are shown in Table 2. The values of k_0 (Table 2) and k_W^{MX} were determined experimentally under appropriate reaction conditions (Table S1, SI, for MX = NaBr). The statistical fitting of the observed data to eq 2 appears to be satisfactory in view of the standard deviations associated with the calculated values of $F_{X/S}$ and $K^{X/S}$ (Table 2) and the plots of Figures S3 (SI) where solid lines are drawn through the calculated data points with residual errors of <5%.

The kinetically effective occurrence of the ion exchange process X^-/S^-, in the related reaction systems,[16,23a] has been found to decrease K_S with the increase of [MX] at a constant $[CTABr]_T$ and temperature, through the empirical relationship

$$K_S = K_S^0/(1 + K_{X/S}[MX]) \quad (3)$$

dx.doi.org/10.1021/jp210467p | J. Phys. Chem. B 2012, 116, 2065−2074

Table 1. Values of k_M and K_S^0, Calculated from Equation 1, for Piperidinolysis of Ionized Phenyl Salicylate (PSa^-)[a]

temp (°C)	$10^3 k_W$[b] (s^{-1})	10^4cmc[c] (M)	10^4cmc[d] (M)	$10^4 k_M$[e] (s^{-1})	K_S^{0e} (M^{-1})	$10^4[CTABr]_T$[f] (M)
40	41.8 ± 0.3[g]	2.0	2.0	43.9 ± 1.1[g]	5322 ± 98[g]	4–500
45	52.6 ± 0.9	3.5	3.4	45.0 ± 0.7	2847 ± 20	4–500
55	56.3 ± 0.4	4.6	4.8	69.9 ± 0.6	1730 ± 94	5–500

[a] $[PSa^-]_0 = 2 \times 10^{-4}$ M, [NaOH] = 0.03 M, [Pip] = 0.10 M, and the aqueous reaction mixture for each kinetic run contained 2% v/v CH_3CN. [b] $k_W = k_{obs}$ at $[CTABr]_T = 0$ [c]The values of cmc were determined from an iterative technique. [d]The values of cmc were determined from a graphical technique. [e]The values of k_M and K_S^0 were calculated from eq 1 by using cmc values obtained from an iterative technique. [f]Total concentration range of CTABr used in the data analysis. [g]Error limits are standard deviations.

Table 2. . Values of Empirical Constants, $F_{X/S}$ and $K^{X/S}$, Calculated from Equation 2 (Where MX = NaBr) in the Presence of CTABr Micelles

temp (°C)	$[CTABr]_T$[a] (M)	$10^4 k_0$[b] (s^{-1})	$F_{X/S}$	$K^{X/S}$ (M^{-1})	$K_{X/S}$[c] (M^{-1})	$K_{X/S}{}^n$[d] (M^{-1})
40	0.005	42.6 ± 0.1[e]	0.74 ± 0.02[e]	1.85 ± 0.11[e]	51.1[f]	37.8
40	0.0125	30.4 ± 0.8	0.58 ± 0.02	0.90 ± 0.07	60.8	35.3
45	0.005	71.2 ± 1.8	0.82 ± 0.02	3.61 ± 0.25	55.0[g]	45.1
45	0.0125	61.7 ± 1.3	0.64 ± 0.01	2.07 ± 0.13	75.7	48.4
55	0.005	110 ± 3.1	0.79 ± 0.01	6.52 ± 0.48	62.9[h]	49.7
55	0.0125	103 ± 2.1	0.58 ± 0.06	4.03 ± 0.18	91.2	52.9

[a]Total concentration of CTABr. [b] $k_0 = k_{obs}$ at [NaBr] = 0. [c] $K_{X/S} = K^{X/S} \times (1 + K_S^0[CTABr]_T)$. [d] $K_{X/S}{}^n = F_{X/S}K^{X/S}$. [e]Error limits are standard deviations. [f] $K_S^0 = 5322\ M^{-1}$. [g] $K_S^0 = 2847\ M^{-1}$. [h] $K_S^0 = 1730\ M^{-1}$.

Table 3. Mean Values of $F_{X/S}$ and K_X^{Br} for M_2X (M_2X = 5-MeSaNa$_2$ or 5-MeOSaNa$_2$) in the Presence of CTABr Micelles

X	temp (°C)	$[M_2X]_0^{op}$	$[M_2X]_{sc}$[a] (M)	$10^2 F_{X/S}$	K_X^{Br} or R_X^{Br}	$\eta(\dot\gamma)^{max}$[b] (mPa·s)	micelles' structure
$MeSa^{2-}$	35	nonzero		92 ± 3[c]	796 ± 48[c]	[d]	V[e,15]
	40	nonzero	0.0125	80 ± 11	358 ± 6	8.6[f]	(V + WM)[e]
	45	nonzero	0.0125	66 ± 9	88 ± 8	35.4	WM[e]
	55	nonzero	0.0125	69 ± 5	53 ± 4	41.1	WM[e]
$MeOSa^{2-}$	35	nonzero	0.02	77 ± 8	89 ± 6	6.5[g]	WM[e]
	40	nonzero	0.02	99.5 ± 1	38 ± 0.1	4.0	WM[e]
	45	nonzero	0.02	96 ± 4	12 ± 1	1.9	WM[e]
	55	nonzero		97 ± 7	7.0 ± 1	[d]	SM[e]

[a]Specific concentration of M_2X at which the viscosity maximum occurs at a constant $\dot\gamma$ and 0.0125 M CTABr. [b]Shear viscosity at $[M_2X]_{sc}$ and constant $\dot\gamma$. [c]Error limits are standard deviations. [d]Absence of well-defined maximum with η not significantly different from η of water. [e]The assignment of the structure of micelles is based upon shear thinning behavior of flow curves obtained for mixed [CTABr]–$[M_2X]$ solutions, M_2X = 5-MeSaNa$_2$ and 5-MeOSaNa$_2$. [f] $\dot\gamma = 21\ s^{-1}$. [g] $\dot\gamma = 11\ s^{-1}$.

where K_S represents the CTABr micellar binding constant of S^- (= PSa^-) and $K_S^0 = K_S$ at [MX] = 0. The magnitude of the empirical constant $K_{X/S}$ is the measure of the ability of counterion X to expel another counterion S from the cationic micellar pseudophase to the aqueous phase through the occurrence of ion exchange X^-/S^- at the cationic micellar surface. It can be easily shown that eqs 1 and 3 can lead to eq 2 with respective k_0, $F_{X/S}$, $k_W{}^{MX}$, and $K^{X/S}$ expressed by eqs 4, 5, and 6[16–19]

$$k_0 = \frac{k_W + k_M K_S^0[CTABr]_T}{1 + K_S^0[CTABr]_T} \quad (4)$$

$$F_{X/S} = \theta / k_W{}^{MX} \quad (5)$$

where $k_W{}^{MX} = k_{obs}$ at $[CTABr]_T = 0$ but $[MX] \neq 0$ and θ is an empirical constant whose value must be $\leq k_W{}^{MX}$ within the domain of the empirical definition of $F_{X/S}$[17a] and

$$K_{X/S} = K_{X/S}(1 + K_S^0[CTABr]_T) \quad (6)$$

The values of $K_{X/S}$ were calculated from eq 6 with known values of K_S^0 (Table 1) and $[CTABr]_T$. These calculated values of $K_{X/S}$, at different $[CTABr]_T$ and temperature, are summarized in Table 2. The values of $K_{X/S}$ are significantly different from each other at 0.005 and 0.0125 M CTABr and at a constant temperature. However, the values of normalized $K_{X/S}{}^n$ (= $F_{X/S}K_{X/S}$) are essentially independent of $[CTABr]_T$, within the limits of their standard deviations, at a constant temperature. These calculated values of $K_{X/S}{}^n$ (for $X = Br^-$), at 40, 45, and 55 °C, are shown in Table 2.

Determination of K_X^{Br} or R_X^{Br} for X = 5-MeSa^{2-} and 5-MeOSa^{2-}. It is evident from Table S1 (SI) that the values of k_{obs} are independent of $[M_2X]$ at ≤0.1 M M_2X for M_2X = 5-MeSaNa$_2$ and 5-MeOSaNa$_2$. Thus, the nonlinear increase of k_{obs} with the increase of $[M_2X]$, as exhibited by the plots of Figures 1 and 2 and Figures S1 and S2 (SI), is attributed to the transfer of PSa^- ions from the cationic micellar pseudophase to the aqueous phase through ion exchange X^-/S^- ($S^- = PSa^-$) because $(k_W/k_M) \geq 10$ (Tables 1–3 and Table S1 (SI)).[16–19] Since the values of k_{obs} remain independent of $[M_2X]$ at $[CTABr]_T = 0$ and $[M_2X] \leq 0.1$ M, the observed data (k_{obs} vs $[M_2X]$) were treated with eq 2 by replacing MX with M_2X and $F_{X/S}k_W{}^{MX}$ with empirical constant θ.[19] The values of θ, $K^{X/S}$, and least-squares, $\sum di^2$, where $di = k_{obsi} - k_{calci}$ with k_{obsi} and k_{calci} representing, respectively, experimentally determined and least-squares calculated rate constants at the ith value of M_2X, were calculated from eq 2 where k_0 was considered as a known parameter determined experimentally at [MX] = 0. The

dx.doi.org/10.1021/jp210467p | J. Phys. Chem. B 2012, 116, 2065–2074

calculated values of θ, $K^{X/S}$, and $\sum di^2$, at different $[CTABr]_T$ and temperature (35−55 °C) for M_2X = 5-MeSaNa$_2$ and 5-MeOSaNa$_2$, are shown in Table S2 (SI).

It is evident from the dashed-line plots of Figures 1 and 2 and Figures S1 and S2 (SI) that the observed data points show significant negative deviations from dashed-lines at the lower values of $[M_2X]$. The absolute magnitudes of the negative deviations increase with the decreasing values of $[M_2X]$. The reasons for these observations have been explained elsewhere.[17a,b,19] These characteristic observations have been attributed to the significant effects of the ion exchange processes X^{2-}/HO^- and X^{2-}/Br^- on k_{obs} under such typical reaction conditions. The consideration of the these independent ion exchange processes has led to eq 7

$$[M_2X]_S^{ef} = [M_2X] - [M_2X]_0^{op} \quad (7)$$

where $[M_2X]_S^{ef}$ represents the effective concentration of M_2X that could affect the ion exchange X^{2-}/S^- (S^- = PSa^-) and $[M_2X]_0^{op}$ is the optimum value of $[M_2X]$ at which the value of $([HO^-_M] + [Br^-_M])$ becomes independent of $[M_2X]$. The values of $[M_2X]_0^{op}$ were calculated by an iterative technique described in the earlier reports.[17a,19] These calculated values of $[M_2X]_0^{op}$, at different values of $[CTABr]_T$ and for M_2X = 5-MeSaNa$_2$ and 5-MeOSaNa$_2$, are shown in Table S2 (SI). The values of θ, $K^{X/S}$, and $\sum di^2$ were also calculated from eq 2 with the replacement of $F_{X/S}k_W^{MX}$ and $[MX]$ by θ and $[M_2X]_S^{ef}$, respectively. These results are also shown in Table S2 (SI). The solid-line plots of Figures 1 and 2 and Figures S1 and S2 (SI), the standard deviations associated with the values of θ and $K^{X/S}$, and the values of $\sum di^2$ (Table S2, SI) reveal that the observed data treatment with eq 2 is more reliable with $[M_2X] = [M_2X]_S^{ef}$ at $[M_2X]_0^{op} \neq 0$ compared with that at $[M_2X]_0^{op} = 0$.

The values of θ or $F_{X/S}$ should be independent of $[CTABr]_T$ as evident from eq 5. Relatively more reliable values of θ or $F_{X/S}$ (Table S2, SI) agree well with this prediction. Thus, the mean values of $F_{X/S}$, at different $[CTABr]_T$ and temperature, are summarized in Table 3 for M_2X = 5-MeSaNa$_2$ and 5-MeOSaNa$_2$.

The values of $K_{X/S}$, at different $[CTABr]_T$, were calculated from eq 6 by using the reported value of K_S^0 (= 7×10^3 M^{-1}) at 35 °C[16,19] and the values of K_S^0 at 40, 45, and 55 °C listed in Table 1. The values of normalized $K_{X/S}^n$ (= $F_{X/S}K_{X/S}$), as shown in Table S2 (SI), are almost independent of $[CTABr]_T$ within its range 5 to ≤ 15 mM. It has been described in the earlier reports[16,17] that the magnitude of $K_{X/S}^n$ is related with CTABr micellar binding constants, K_X and K_S, of respective counterions X and S (= PSa^-) by the relationship: $K_{X/S}^n = \Omega_S K_X/K_S$ where Ω_S is the proportionality constant. Similarly, for another reference/standard counterion Br, $K_{Br/S}^n = \Omega_S K_{Br}/K_S$. If the values of $K_{X/S}^n$ and $K_{Br/S}^n$ were determined in the presence of micelles of identical structural features such as spherical or rodlike/wormlike micelles or vesicles, then the relationships $K_{X/S}^n = \Omega_S K_X/K_S$ and $K_{Br/S}^n = \Omega_S K_{Br}/K_S$ can lead to eq 8

$$K_X/K_{Br} = K_{X/S^n}/K_{Br/S^n} \quad (8)$$

where K_X/K_{Br} (≡ K_X^{Br}) represents the usual ion exchange constant, i.e., $K_X^{Br} = ([X_M][Br_W])/([X_W][Br_M])$. However, if the values of $K_{X/S}^n$ and $K_{Br/S}^n$ were determined in the presence of respective nonspherical and spherical micelles, then K_X/K_{Br} (≡ R_X^{Br}) of eq 8 represents the ratio of the CTABr micellar binding constants K_X (determined in the presence of nonspherical micelles) and K_{Br} (determined in the presence of spherical micelles).The relationship $(K_{X/S}^n/K_{Br/S}^n) = R_X^{Br}$ is correct only if the assumption that the values of Ω_S/K_S remain independent of the micellar structural features.

The calculated values of $K_{X/S}^n$ summarized in Table S2 (SI), the values of $K_{Br/S}^n$ at 40, 45, and 55 °C (Table 2), and the reported value of $K_{Br/S}^n$ (= 25 M^{-1}) at 35 °C[19,23a] were used to calculate K_X/K_{Br} (≡ K_X^{Br} or R_X^{Br}) from eq 8. These results, at different $[CTABr]_T$ (0.005 to ≤ 0.015 M) and temperature (35−55 °C) for M_2X = 5-MeSaNa$_2$ and 5-MeOSaNa$_2$, are summarized in Table S2 (SI). It is noteworthy that the value of $K_{Br/S}^n$ (= 25 M^{-1} at 35 °C) has been derived from the kinetic parameters obtained in the presence of spherical micelles.[19,23a] Thus, the values of $K_{Br/S}^n$ at 40, 45, and 55 °C (Table 2) should be expected to be derived from the kinetic parameters obtained in the presence of spherical micelles. The calculated values of K_X^{Br} or R_X^{Br} are almost independent of $[CTABr]_T$ within its range 0.005 to ≤0.015 M, and therefore the mean values of K_X^{Br} or R_X^{Br} for X = 5-MeSa^{2-} and 5-MeOSa^{2-} are shown in Table 3.

The mean value of R_X^{Br} (= 89) for X = 5-MeOSa^{2-} is nearly 2-fold larger than that for X = salicylate dianion (Sa^{2-}).[28] These observations reveal that apparent hydrophobicity of 5-MeOSa^{2-} is larger than that of Sa^{2-}. However, the value of K_X^{Br} for X = $C_6H_5CO_2^-$ (K_X^{Br} = 5.0, 5.8,[16] 5.9[29]) is similar to that for X = 4-MeO$C_6H_4CO_2^-$ (K_X^{Br} = 5.2[16]). These results show that the apparent hydrophobicity of $C_6H_5CO_2^-$ is not appreciably different from that of 4-MeO$C_6H_4CO_2^-$. Since the ether groups such as polyoxyethylene groups constitute hydrophilic head groups of a large number of nonionic surfactants, it is obvious to question "Is the ether group hydrophilic or hydrophobic?" In search of an answer to such a question, Menger and Chlebowski[30] carried out a systematic and detailed study where they concluded that two ether groups, attached to the tails of the cationic surfactants, were not sufficiently hydrophilic to prevent aggregation. However, the two ether groups managed to alter the micelles' morphology and properties considerably.[30] The value of R_X^{Br} for X = 4-Me$C_6H_4CO_2^-$ is 17[17a] which is 3.3-fold larger than that for X = 4-MeO$C_6H_4CO_2^-$. However, the values of R_X^{Br} are 7.5-, 7.1-, 9.5-, and 9.0- fold larger for X = 5-MeSa^{2-} than the corresponding values for X = 5-MeOSa^{2-} at 55, 45, 40, and 35 °C, respectively.

Explanation of Rheometric Observations. The flow curves, at ≥0.01 M 5-MeSaNa$_2$, 0.0125 M CTABr, and 35 °C, exhibit Newtonian fluid systems, while flow curves at ≤0.007 M 5-MeSaNa$_2$ show a weak but definite shear thickening behavior (Figure 3a and Figure S5, SI). Similar rheological observations but with comparatively low values of η were also obtained at 0.005 M CTABr and 35 °C (Figure S7a, SI). Most of the flow curves of Figures 3b and 4 as well as Figures S5, S6a, and S6b (SI), at ≥0.01 M M_2X, M_2X = 5-MeSaNa$_2$ and 5-MeOSaNa$_2$, exhibit shear thinning which is a typical characteristic of the presence of wormlike micelles in surfactant solutions containing a fixed concentration of micelle-forming surfactant and varying values of [MX].[31−33] However, the Newtonian behavior of flow curves of Figure 3b, at ≥0.04 M 5-MeSaNa$_2$, and Figure 4, at 0.1 M 5-MeOSaNa$_2$, may be attributed to the presence of branched micelles. The flow curves (Figures 3a, 3b, and Figure 4 as well as Figures S5a, S5b, S6a, and S6b, SI), showing weak shear thickening behavior at ≤0.007 M M_2X, M_2X = 5-MeSaNa$_2$ and 5-MeOSaNa$_2$, are indicative of the presence of probable spherical micelles, SM, in CTABr−M_2X solutions.[19] The Newtonian flow curves of Figure S6c (SI) reveal the

dx.doi.org/10.1021/jp210467p | J. Phys. Chem. B 2012, 116, 2065−2074

presence of only probable SM in 0.0125 M CTABr−≤0.1 M $MeOSaNa_2$ mixtures at 55 °C, but the Newtonian behavior of flow curves of Figure 3a and Figure S7a (SI) at ≥0.01 M 5-$MeSaNa_2$ shows the presence of ULV.[11] The flow curves of Figures S5a and S5b (SI) reveal the presence of probable branched micelles at ≥0.04 M 5-$MeSaNa_2$. However, It appears that the Newtonian behavior of flow curves for ULV is indistinguishable from that for probable branched micelles at ≥0.04 M 5-$MeSaNa_2$. The flow curves, obtained at ≤0.007 M 5-$MeSaNa_2$ and within the temperature range 35−55 °C, indicate that the extent of shear thickening behavior decreases with the increasing temperature. It is perhaps noteworthy that the value of η of 0.024 Pa·s at $\dot{\gamma}$ = 21 s^{-1} and 55 °C is not appreciably different from the corresponding value of 0.030 Pa·s obtained from ref 15 where, instead of 5-$MeSaNa_2$, 5-MeSaH was used.

The plots of shear viscosity at a constant shear rate, $\dot{\gamma}$ (= 21 s^{-1}), i.e., $\eta(\dot{\gamma})$ vs $[M_2X]$, at different temperatures for M_2X = 5-$MeSaNa_2$ are shown in Figure 5a. Well-defined maxima of the plots, at 40, 45, and 55 °C, occur at the same value of $[M_2X]$

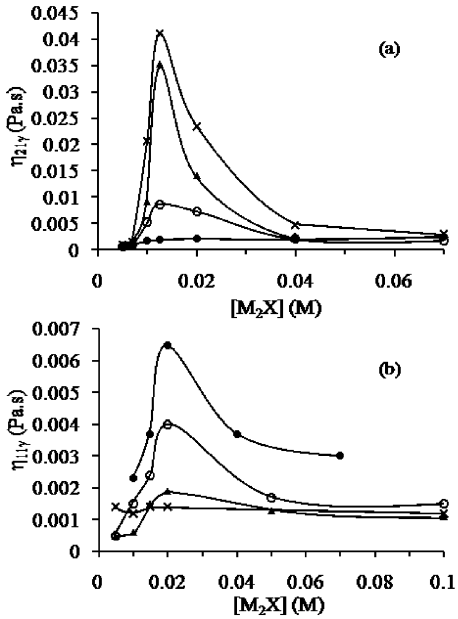

Figure 5. Plots of shear viscosity at a constant shear rate (i.e., η_γ) vs $[M_2X]$ at 35 °C (●), 40 °C (○), 45 °C (▲), and 55 °C (×) for (a) M_2X = 5-$MeSaNa_2$, $\dot{\gamma}$ = 21 s^{-1} and (b) M_2X = 5-$MeOSaNa_2$, $\dot{\gamma}$ = 11 s^{-1}.

(i.e., $[M_2X]_{sc}$ = 0.0125 M), while the values of $\eta(\dot{\gamma})$ at $\dot{\gamma}$ = 21 s^{-1} and 35 °C increase nonlinearly from 0.6 to 2.5 mPa·s with the increase of $[M_2X]$ from 0.005 to 0.07 M. The values of $[M_2X]_{sc}$, specific concentration of M_2X at which the viscosity maximum occurs at a constant $\dot{\gamma}$ and [CTABr], remained unchanged within the temperature range 40−55 °C at $\dot{\gamma}$ values of 21, 505, and 10^3 s^{-1}. The plots of $\eta(\dot{\gamma})$ ($\dot{\gamma}$ = 21 s^{-1}) vs $[M_2X]$ for M_2X = 5-$MeSaNa_2$, at 55 °C and 0.005 as well as 0.0125 M CTABr, are shown in Figure S8 (SI). The value of $[M_2X]_{sc}$ changed from 0.0125 to 0.007 M with the change of [CTABr] from 0.0125 to 0.005 M at 55 °C. The plot of zero shear viscosity (η_0) vs [5-MeSaH] at 0.0125 M CTABr and 25 °C combined with turbidimetry measurements revealed the presence of probable ellipsoidal micelles,[14] WM and ULV at ≤0.005, >0.005, and ≥0.015 M 5-MeSaH, respectively.[15] However, in the present study, the presence of probable SM at ≤0.007 M 5-$MeSaNa_2$, within the temperature range 35−55 °C, may be attributed to the nature of counterionic salt 5-$MeSaNa_2$ instead of 5-MeSaH. It is evident from Figure S7b and Figure S8 (SI) that, at 0.005 M CTABr, the lowest values of $[M_2X]$ at which wormlike micelles start to form are in the range >0.002 to <0.005 M at 55 °C. The plots of Figure 5a show that the value of $[MX]_{sc}/[CTABr]_T$ is 1.0 which is not appreciably different from the corresponding value of 0.98 obtained with 5-MeSaH.[15]

The plots of $\eta(\dot{\gamma})$ ($\dot{\gamma}$ = 11 s^{-1}) vs $[M_2X]$ (M_2X = 5-$MeOSaNa_2$) at 35, 40, 45, and 55 °C reveal the presence of the maxima at 0.02 M M_2X (Figure 5b), i.e., $[M_2X]_{sc}/[CTABr]_T$ = 1.6. The positions of maxima (i.e., the values of $[M_2X]_{sc}$) remained unchanged at $\dot{\gamma}$ of 11, 505, and 10^3 s^{-1} and at a constant temperature within its range 35−45 °C (Figure 5b). Although the presence of, at least, a single maximum in the plot of $\eta(\dot{\gamma})$ vs [MX] for aqueous solutions containing cationic surfactants and their counterionic salts, MX, is no longer unusual,[15,34] the molecular mechanism for the origin of such a maximum is far from being understood even at a rudimentary molecular level.[15,35] However, it has become almost certain from several experimental studies[15,34] that the occurrence of a viscosity maximum for a surfactant solution containing a constant concentration of ionic micelle-forming surfactant and different concentration of MX is indicative of the existence of WM/entangled WM in the surfactant solutions. It is perhaps noteworthy that a significantly lower value of $\eta(\dot{\gamma})^{max}$ at 40 °C than that at 45 °C for 5-$MeSaNa_2$ reveals the presence of ULV along with WM at 40 °C. However, the satisfactory observed data fit to eq 2, as evident from the plots of Figure S1 (SI), show that either the value of R_X^{Br} for WM is not significantly different from that for ULV or the presence of WM is not significant enough to cause a detectable deviation of observed data fit to eq 2 at 40 °C.

Rheometric measurements revealed the presence of unilamellar vesicles (ULV) and WM at 35 and 55 °C, respectively, for 0.0125 M CTABr → 0.007 M 5-$MeSaNa_2$ mixtures. The value of R_X^{Br} (for ULV)/R_X^{Br} (for WM) is 15 (= 796/53). Davies et al.[15] have proposed a tentative mechanism of ULV-to-WM transition in CTABr−5-MeSaH mixtures where 5-MeSaH molecules exist in fully nonionized form. This mechanism suggests that the change in the value of $[CTABr_{M/V}]/[5MeSaH_{M/V}]$, where $CTABr_{M/V}$ and $5\text{-}MeSaH_{M/V}$ represent micelle- or/ULV-bound respective CTABr and 5-MeSaH molecules, from 1.0 to <1.0 causes the change of structure of aggregates from WM to ULV. This proposed mechanism thus indirectly implies that the value of cationic micellar binding constant ($K_{5\text{-MeSaH}}$) of 5-MeSaH should be larger in the presence of ULV than that of WM. The present study provides a quantitative measure of this proposal although 5-MeSaH, used in the study,[15] differs from 5-$MeSaNa_2$ in terms of the state of ionization of OH and CO_2H groups.

It has been a general perception, although based upon merely qualitative experimental observations, that the selective and strong counterion binding to ionic micelles results in micellar structural transition from short rodlike (RM) to long stiff and flexible RM/WM to entangled and branched/multiconnected micelles.[2,15,34d,35−38] Recently, it has been shown that benzoate and substituted benzoate ions (X) with K_X^{Br} values of <6.0, when mixed with <0.07 M CTABr or CTAX and with or without varying concentration of X at 25 or 35 °C, form only SM.[23,33,34] However, aqueous solutions containing 0.015 M

dx.doi.org/10.1021/jp210467p | J. Phys. Chem. B 2012, 116, 2065−2074

CTABr and varying values of [NaX] reveal the presence of short RM when K_X^{Br} = 9.0 as well as long linear flexible, entangled, and branched WM when the values of K_X^{Br} range from ~13 to 71 at 35 °C.[19,27] The increase in temperature from 35 to 55 °C decreased R_X^{Br} from 796 to 53 for X = 5-MeSa^{2-} and from 89 to 7.0 for X = 5-MeOSa^{2-} (Table 3). Rheometric measurements on 0.0125 M CTABr to ≥0.01 M M_2X mixtures showed the presence of ULV and long linear, entangled, branched WM for M_2X = 5-MeSaNa$_2$ at 35 and 55 °C, respectively. Thus, these observations reveal the presence of (i) long linear, entangled, branched WM when R_X^{Br} = 53−88 (for X = 5-MeSa^{2-}) and 89 (for X = 5-MeOSa^{2-}), (ii) ULV when R_X^{Br} = 796 (for X = 5-MeSa^{2-}), and (iii) probable SM when K_X^{Br} or R_X^{Br} = 7.0 (for X = 5-MeOSa^{2-}).

Figure 6 shows the variations in R_X^{Br} as well as shear viscosity ($\eta(\dot{\gamma})$) at $\dot{\gamma}$ = 21 s^{-1} as a function of temperature (within the 35−55 °C range) at C_s/C_d = 1.0 (Figure 6a) where C_s = [5-MeSaNa$_2$] and C_d = [CTABr]$_T$ and C_s/C_d = 1.6 (Figure 6b) with a fixed value of C_d (= 0.0125 M). The increase in temperature caused nonlinear increase and decrease in $\eta(\dot{\gamma})$ and R_X^{Br}, respectively, at both values of C_s/C_d. Similarly, Davies et al.[11] reported the increase in η_0 with the increase in temperature from 45 to 55 °C at C_s'/C_d = 1.6 with C_d = 0.0125 M where C_s' represents 5-methylsalicylic acid (5-MeSaH = 5-Me-2-HO-C$_6$H$_3$CO$_2$H). Rheometric measurements showed that the temperature ranges 35−45 °C (Figures 3a, 3b) and 45−55 °C[15] represent the micellar structural transition from ULV to WM. The increase in temperature generally decreases η_0[39] or $\eta(\dot{\gamma})$ (at considerably low values of $\dot{\gamma}$) as evident from the viscosity peak of the plot of η_0 vs temperature at the constant concentration of counterionic salt.[15,40] The most plausible cause for the increase in $\eta(\dot{\gamma})$ or η_0[15] with increasing temperature (Figure 6a, 6b) and ref 15 may be attributed to the presence of both vesicles and WM in different proportions under such typical temperature range. Figure 6c shows the changes in R_X^{Br} or K_X^{Br} (where X = 5-MeOSa^{2-}) as well as shear viscosity at $\dot{\gamma}$ = 11 s^{-1}, $[M_2X]_{sc}$ = 0.02, and 0.0125 M CTABr, i.e., $\eta(\dot{\gamma})^{max}$, as a function of temperature. The increase of temperature from 35 to 55 °C caused a nonlinear decrease of both R_X^{Br} and $\eta(\dot{\gamma})^{max}$. The plot of R_X^{Br} vs $\eta(\dot{\gamma})^{max}$ (not shown) appears to be linear with positive slope.

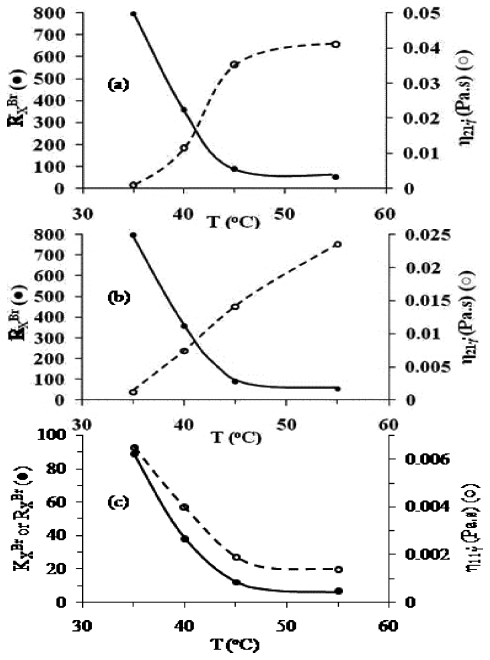

Figure 6. Plots showing the dependence of R_X^{Br} (●) and shear viscosity at 21 s^{-1} shear rate, $\eta_{21\gamma}$ (○), upon temperature where (a) [CTABr]$_T$ = [5-MeSaNa$_2$] = 0.0125 M and (b) [CTABr]$_T$ = 0.0125 M and [5-MeSaNa$_2$] = 0.02 M. (c) Plots showing the dependence of R_X^{Br} or K_X^{Br} (●) and $\eta_{11\gamma}$ (○) upon temperature at 0.02 M 5-MeOSaNa$_2$ and 0.0125 M CTABr.

It is interesting to note that Figure 6c, perhaps for the first time, reveals an approximate linear increase in $\eta(\dot{\gamma})^{max}$ with the increase of R_X^{Br} caused by the decrease in temperature from 45 to 35 °C at constant [5-MeOSaNa$_2$] = 0.02 M and [CTABr] = 0.0125 M. It is evident from these observations that, at a constant [CTABr], the micellar structural transitions from probable SM to short stiff RM to long linear, entangled, branched WM to ULM may be correlated quantitatively with the magnitudes of R_X^{Br} regardless of whether such micellar structural transitions occur due to variation in [MX] or [M_2X] at a constant temperature or due to variation in temperature at a constant [MX] or [M_2X].

The probable answer to a question on how counterion affinity to ionic micelles affects the structure of aggregates of aqueous ionic surfactants may be derived from the definition of the hydrophobic interaction. It is perhaps tempting to argue that the release of some micellized water molecules during the micellar structural transition from SM to RM[9b] is the consequence of the fundamental definition of the so-called hydrophobic interaction which may be briefly described as follows. A solubilizate molecule is said to solubilize in water solvent when the absolute value of solvation energy (i.e., energy released due to formation of solvation shell around solubilizate molecule) becomes equal to or larger than the energy required to form a cavity in the three-dimensional structural network of the water solvent for embedment of the solubilizate molecule. A surfactant molecule consists of both hydrophobic and hydrophilic molecular segments. When the hydrophobic segment becomes considerably larger than voids in the three-dimensional structural network of water solvent and solvation energy for a single molecule is not sufficient to counterbalance the energy needed to form a cavity for embedding the molecule, then surfactant molecules begin to aggregate because it is energetically less expensive or easier to form a larger cavity than more than one relatively smaller one to embed the same n number of solubilizate molecules. This process of aggregation of surfactant molecules is referred to as so-called hydrophobic interaction. Since the surfactant molecules contain both hydrophilic segments (called headgroups) and hydrophobic segments (generally long methylene chains C_nH_{2n+1} with n > 8), packing of headgroups and tails during the formation of a micelle involves different molecular interactions in terms of energetics. In view of the definition of hydrophobic interaction, the increase of the hydrophobic segment compared with the hydrophilic segment of micelle should decrease the value of R_W^{Sur} = [H_2O_M]/[Sur_M] where [H_2O_M] and [Sur_M] represent the respective concentration of micellized H_2O and Sur (= surfactant) molecules. Thus, the value of R_W^{Sur} should vary in the order: R_W^{Sur} (for SM) > R_W^{Sur} (for SRM) > R_W^{Sur} (for LRM) > R_W^{Sur} (for WM) > R_W^{Sur} (for Vs = vesicle) where SRM and LRM represent respective short and long stiff RM. Similarly, the value of counterion (X) binding constant (K_X) with ionic micelles/vesicles should vary in the order: K_X (for

dx.doi.org/10.1021/jp210467p | J. Phys. Chem. B 2012, 116, 2065−2074

SM) < K_X (for SRM) < K_X (for LRM) < K_X (for WM) < K_X (for Vs).

CONCLUSIONS

The selectivity of binding of counterions to ionic interfaces remains an important but unsolved problem in many areas of colloid and interface science. Recently, Romsted has pointed out in an invited feature article[9b] that identifying and quantifying the interactions that control aggregate morphologies of amphiphiles, in particular ion-specific interactions, remain unsolved problems both experimentally and theoretically. The new aspect of the present manuscript is the experimentally determined values of K_X^{Br} or R_X^{Br} for X = 5-MeSa^{2-} and 5-MeOSa^{2-} at 35, 40, 45, and 55 °C as well as within the $[CTABr]_T$ range 0.005 to ≤0.015 M. Rheometric measurements of 0.0125 M CTABr to ≥0.01 M 5-MeSaNa$_2$ reveal the presence of ULV and WM at 35 and ≥45 °C, respectively. The notable features of these observations are the quantitative correlation between counterionic (X) affinity of cationic micelles (measured by the value of K_X^{Br} or R_X^{Br}) and the [X]-induced micellar structural transition from probable SM-to-RM/WM-to-ULV. A quantitative correlation is capable of predicting the structures of molecular aggregates, formed in aqueous solutions containing 15 mM CTABr and different concentrations of MX, based upon the numerical values of R_X^{Br}, while a qualitative correlation lacks such a capability. Similarly, perhaps for the first time, a quantitative correlation between temperature-affected values of R_X^{Br} and temperature-induced micellar structural transitions has been also achieved.

ASSOCIATED CONTENT

Supporting Information

Derivation of eq 1, Appendix, Tables S1 and S2 and Figures S1−S8. This material is available free of charge via the Internet at http://pubs.acs.org.

AUTHOR INFORMATION

Corresponding Author

*E-mail: niyaz@um.edu.my. Tel.: +603 7967 4163. Fax: +603 7967 4193.

Notes

The authors declare no competing financial interest.

ACKNOWLEDGMENTS

We thank the Ministry of Higher Education (MOHE), University of Malaya (UM), for financial assistance through research grants UM.C/HIR/MOHE/SC/07 and RG022/09AFR and the centre of Ionic Liquids, UM, for permission to carry out the rheological study.

REFERENCES

(1) Gravsholt, S. *J. Colloid Interface Sci.* **1976**, *57*, 575−577.
(2) Rao, U. R. K.; Manohar, C.; Valaulikar, B. S.; Iyer, R. M. *J. Phys. Chem.* **1987**, *91*, 3286−3291.
(3) Penfold, J.; Tucker, I.; Staples, E.; Thomas, R. K. *Langmuir* **2004**, *20*, 8054−8061.
(4) Vermuthen, M.; Stiles, P.; Bachofer, S. J.; Simonis, U. *Langmuir* **2002**, *18*, 1030−1042.
(5) Oelschaeger, C.; Schopferer, M.; Scheffold, F.; Willenbacher, N. *Langmuir* **2010**, *26*, 7045−7053.
(6) Singh, K.; Marangoni, D. G.; Quinn, J. G.; Singer, R. D. *J. Colloid Interface Sci.* **2009**, *335*, 105−111.
(7) Kunz, W.; Henle, J.; Ninham, B. W. *Curr. Opin. Colloid Interface Sci.* **2004**, *9*, 19−37 and references cited therin.
(8) (a) Vlachy, N.; Jagoda-Cwiklik, B.; Vacha, R.; Touraud, D.; Jungwirth, P.; Kunz, W. *Adv. Colloid Interface Sci.* **2009**, *146*, 42−47. (b) Klein, R.; Kellermeier, M; Drechsler, M.; Touraud, D.; Kunz, W. *Colloids Surf. A* **2009**, *338*, 129−134. (c) Abezgauz, L.; Kuperkar, K.; Hassan, P. A.; Ramon, O.; Bahadur, P.; Danino, D. *J. Colloid Interface Sci.* **2010**, *342*, 83−92.
(9) (a) Geng, Y.; Romsted, L. S.; Menger, F. *J. Am. Chem. Soc.* **2006**, *128*, 492−501. (b) Romsted, L. S. *Langmuir* **2007**, *23*, 414−424 and references cited therein.
(10) Lin, Z.; Cai, J. J.; Scriven, L. E.; Davis, H. T. *J. Phys. Chem.* **1994**, *98*, 5984−5993.
(11) Zheng, Y.; Lin, Z.; Zakin, J. L.; Talmon, Y.; Davis, H. T.; Scriven, L. E. *J. Phys. Chem. B* **2000**, *104*, 5263−5271.
(12) Buwalda, R. T.; Stuart, M. C. A.; Engberts, J. B. F. N. *Langmuir* **2000**, *16*, 6780−6786.
(13) Hassan, P. A.; Valaulikar, B. S.; Manohar, C.; Kern, F.; Bourdieu, L.; Candau, S. J. *Langmuir* **1996**, *12*, 4350−4357.
(14) One of the reviewers has pointed out that it is never justified that strictly spherical micelles are formed in this particular system.
(15) Davies, T. S.; Ketner, A. M.; Raghavan, S. R. *J. Am. Chem. Soc.* **2006**, *128*, 6669−6675.
(16) Khan, M. N. Micellar Catalysis. In *Surfactant Science Series*; CRC Press: Boca Raton, FL, 2006; Vol. *133* and references cited therein.
(17) (a) Khan, M. N. *Adv. Colloid Interface Sci.* **2010**, *159*, 160−179. (b) Khan, M. N.; Ismail, E. *J. Mol. Liq.* **2007**, *136*, 54−63. (c) Khan, M. N.; Sinasamy, S. *Int. J. Chem. Kinet.* **2011**, *43*, 9−20.
(18) Khan, M. N.; Ismail, E. *J. Phys. Chem. A* **2009**, *113*, 6484−6488.
(19) Yusof, N. S. M.; Khan, M. N. *Langmuir* **2010**, *26*, 10627−10635 and references cited therein..
(20) Khan, M. N.; Gambo, S. K. *Int. J. Chem. Kinet.* **1985**, *17*, 419−428.
(21) (a) Khan, M. N. *J. Chem. Soc., Perkin Trans. 2* **1989**, 199−208. (b) Khan, M. N. *J. Org. Chem.* **1983**, *48*, 2046−2052.
(22) Khan, M. N. *J. Chem Soc., Perkin Trans. 2* **1990**, 445−457.
(23) (a) Khan, M. N.; Arifin, Z.; Lasidek, M. N.; Hanifiah, M. A. M.; Alex, G. *Langmuir* **1997**, *13*, 3959−3964. (b) Khan, M. N.; Arifin, Z.; Ismail, E.; Ali, S. F. M. *J. Org. Chem.* **2000**, *65*, 1331−1334.
(24) Khan, M. N.; Ismail, E. *Int. J. Chem. Kinet.* **2001**, *33*, 288−294.
(25) Khan, M. N.; Arifin, Z. *J. Colloid Interface Sci.* **1996**, *180*, 9−14.
(26) Broxton, T. J.; Christie, J. R.; Chung, R. P.-T. *J. Org. Chem.* **1988**, *53*, 3081−3084.
(27) Yusof, N. S. M.; Khan, M. N. *J. Colloid Interface Sci.* **2011**, *357*, 121−128.
(28) Khan, M. N.; Ismail, E.; Yusof, N. S. M. *Colloids Surf. A* **2010**, *361*, 150−161.
(29) Khan, M. N.; Ismail, E. *J. Dispersion Sci. Technol.* **2010**, *31*, 314−320.
(30) Menger, F. M.; Chlebowski, M. E. *Langmuir* **2005**, *21*, 2689−2695.
(31) Qiao, Y.; Lin, Y.; Wang, Y.; Li, Z.; Huang, J. *Langmuir* **2011**, *27*, 1718−1723.
(32) Lu, T.; Huang, J.; Li, Z.; Jia, S.; Fu, H. *J. Phys. Chem. B* **2008**, *112*, 2909−2914.
(33) Raghavan, S. R.; Kaler, E. W. *Langmuir* **2001**, *17*, 300−306.
(34) (a) Rehage, H.; Hoffmann, H. *Mol. Phys.* **1991**, *74*, 933−973. (b) Driess, C. A. *Soft Matter* **2007**, *3*, 956−970 and references cited therein. (c) Lin, Y.; Qiao, Y.; Yan, Y.; Huang, J. *Soft Matter* **2009**, *5*, 3047−3053. (d) Oelschlaeger, C.; Schopferer, M.; Scheffold, F.; Willenbacher, N. *Langmuir* **2009**, *25*, 716−723. (e) Schubert, B. A.; Wagner, N. J.; Kaler, E. W.; Raghavan, S. R. *Langmuir* **2004**, *20*, 3564−3573. (f) Ali, A. A.; Makhloufi, R. *Colloid Polym. Sci.* **1999**, *277*, 270−275. (g) Abdel-Rahem, R. *Adv. Colloid Interface Sci.* **2008**, *141*, 24−36 and references cited therein.
(35) Ziserman, L.; Abezgauz, L.; Ramon, O.; Raghavan, S. R.; Danino, D. *Langmuir* **2009**, *25*, 10483−10489.
(36) Qi, Y.; Zakin, J. L. *Ind. Eng. Chem. Res.* **2002**, *41*, 6326−6336.

(37) (a) Carver, M.; Smith, T. L.; Gee, J. C.; Delichere, A.; Caponetti, E.; Magid, L. J. *Langmuir* **1996**, *12*, 691−698. (b) Magid, L. J.; Han, Z.; Warr, G. G.; Cassidy, M. A.; Butler, P. D.; Hamilton, W. A. *J. Phys. Chem. B* **1997**, *101*, 7919−7927.
(38) Ali, A. A; Makhloufi, R. *Colloid Polym. Sci.* **1999**, *277*, 270−275.
(39) Kuperkar, K.; Abezgauz, L.; Danino, D.; Verma, G.; Hassan, P. A.; Aswal, V. K.; Varade, D.; Bahadur, P. *J. Colloid Interface Sci.* **2008**, *323*, 403−409.
(40) Hassan, P. A.; Valaulikar, B. S.; Manohar, C.; Kern, F.; Bourdieu, L.; Candau, S. J. *Langmuir* **1996**, *12*, 4350−4357.